Diagn Interv Radiol 2017; 23:100–105

ABDOMINAL IMAGING

ORIGINAL ARTICLE

Comparison of biexponential and monoexponential DWI in evaluation of Fuhrman grading of clear cell renal cell carcinoma

Lijuan Shen
Liangping Zhou
Xiaohang Liu
Xiaoqun Yang

PURPOSE
Clear cell renal cell carcinoma (ccRCC) is the most common primary malignant urologic tumor. The Fuhrman grading system is an independent indicator for aggressiveness and prognosis of ccRCC. We aimed to assess the possible diagnostic role of biexponentially and monoexponentially fitted signal attenuation for the Fuhrman grading.

METHODS
A total of 33 patients with ccRCC underwent multiple b values (0, 20, 50, 100, 150, 250, 400, 600, 800, 1000 s/mm^2) diffusion-weighted imaging (DWI). Biexponential parameters (fast ADC [ADCf], slow ADC [ADCs], and fraction of ADCf [*f*]) and monoexponential apparent diffusion coefficient were calculated, and correlated with the Fuhrman grade of ccRCC respectively. The performance of biexponential parameters in differentiating Fuhrman low- and high-grade tumors was assessed and compared with ADC value by receiver operating characteristic analysis.

RESULTS
Qualified images and diffusion-weighted parameters were obtained for all patients. The ADCf and *f* value were positively correlated, whereas ADCs and ADC value were negatively correlated with Fuhrman grade. Significant differences were observed in ADCf ($P < 0.001$), ADCs ($P = 0.005$), and *f* values ($P < 0.001$) of high- and low-grade ccRCCs. When differentiating Fuhrman low-grade tumors from high-grade, the ADCf revealed an area under receiver operating characteristic curve of 0.959, which was higher than the ADC value (0.789; $P = 0.046$), while ADCs (0.807) and *f* (0.833) showed no significant difference from ADC ($P = 0.85$ for ADCs, $P = 0.73$ for *f*).

CONCLUSION
Biexponential DWI provides additional parameters for ccRCC. ADCf is more accurate compared with the ADC value in characterizing Fuhrman grade of ccRCC.

Renal cell carcinoma (RCC) is the most common renal carcinoma in adults, accounting for 85% of all renal cancers (1, 2). The Fuhrman nuclear grade system is the most widely adopted nuclear grading system for clear cell RCC (ccRCC), and is an independent indicator for aggressiveness and prognosis (3). Although the majority of tumors can be cured by surgery at the time of diagnosis, assessment of tumor aggressiveness is meaningful for decisions regarding the optimal surgical intervention, such as the applicability of nephron sparing surgery (4). Thus, a precise diagnosis of preoperative Fuhrman grade becomes sufficiently important. As noninvasive assessment modalities, computed tomography (CT) and magnetic resonance imaging (MRI) have been used to determine therapeutic strategies and surgical planning in RCC (5–18).

It is noteworthy that diffusion-weighted imaging (DWI), combined with various mathematical models, was reported as an effective technique in some studies (8–18). Currently, the monoexponential DWI refers to a widely used mathematical model of clinical DWI. Apparent diffusion coefficient (ADC) value, a monoexponential parameter, is a useful tool to diagnose benign or malignant tumors, RCC subtypes, and Fuhrman nuclear grading of tumors (8–14). The biexponential DWI signal decay with increasing b-values in a large range is a new model designed in recent years. Many researchers revealed that biexponential decay functions was a better model of signal decay, and could enable an independent analysis of the characteristics of ADC values and their interrelationships (15–22). The biexponential parameters include ADCf (the fast components of ADC), ADCs (the slow components of ADC), and *f* (the fraction of ADCf). ADCf represents pseudo-diffusion, which is associated with blood flow in

From the Department of Radiology (L.S.), The Fifth People's Hospital of Shanghai, Fudan University, Shanghai, China; the Departments of Radiology (L.Z. ✉ *25278721@qq.com*, X.L.) and Pathology (X.Y.), Shanghai Cancer Center, Fudan University, Shanghai, China.

Received 14 December 2015; revision requested 25 January 2016; last revision received 26 July 2016; accepted 28 July March 2016.

Published online 4 January 2017.
DOI 10.5152/dir.2016.15519

the microvasculature of random orientation, determined predominantly by low b values; ADCs represents tissue diffusivity, which refers to the true tissue diffusion; and *f* value represents the fraction of ADCf (22). Although biexponential DWI model was successfully applied in previous studies involving the brain and prostate (19–22), it was rarely used for RCC (15–18).

The present study aimed to analyze the correlation between biexponential DWI parameters (ADCf, ADCs, and *f*) and Fuhrman nuclear grading, as well as the performance of each parameter in discriminating high or low Fuhrman grading compared with the monoexponential DWI parameter, ADC.

Methods

Clinical information

From June 2012 to February 2013, forty-eight patients with renal masses suspicious for ccRCC were enrolled in our study. All patients without invasive examinations (such as biopsy, fine-needle aspiration) within three days underwent an MRI examination including DWI at multiple b values. Following the MRI exam, 41 patients received surgerical treatment within two weeks, while seven patients did not. Pathologic examinations confirmed the diagnosis of ccRCC in 35 patients, angiomyolipoma in four, and chromophobe cell carcinoma in two. Two patients were excluded, as their mainly cystic lesions exceeded the range of the calculation of ADCf and *f* value. Therefore, a total of 33 patients with ccRCC and qualified images were included in the analysis (Table 1). All pathologic results were reviewed by a senior pathologist. The Fuhrman nuclear grading of the tumor was determined by the high-level segment when renal cell carcinoma displayed uneven grades in microscope due to heterogeneity of the tumor. The study protocol was institutional review board approved, and written informed consents were obtained from all patients.

Table 1. Pathologic findings and qualified images

Pathologic types	Nephrectomy specimen/ biopsy	Qualified images*	Median age (range), yrs	Male/female
Angiomyolipoma	3/1	-	57 (52–65)	1/3
Chromophobe cell carcinoma	2/0	-	39.5 (31–68)	1/1
ccRCC Fuhrman grade 1	2/0	1	60	1/0
ccRCC Fuhrman grade 2	14/0	14	52 (30–68)	7/7
ccRCC Fuhrman grade 3	17/0	16	63 (40–75)	12/4
ccRCC Fuhrman grade 4	2/0	2	56.5 (51–62)	2/0

ccRCC, clear cell renal cell carcinoma.
*Qualified images refers to lesions that are not cystic for the most part and do not encompass large regions exceeding the range of calculation.

Main points

- The monoexponential and biexponential diffusion-weighted imaging (DWI) might be helpful to characterize Fuhrman grade of clear cell renal cell carcinoma (ccRCC).
- The monoexponential and biexponential diffusion parameters were correlated with Fuhrman nuclear grading; biexponential parameter fast apparent diffusion coefficient (fADC) value had the highest correlation coefficient.
- The biexponential DWI provides additional parameters for differentiating Fuhrman low-grade ccRCC from high-grade ccRCC; ADCf showed relatively higher diagnostic sensitivity and specificity compared with the ADC value.

Image acquisition

All scans were performed using 3.0 T MRI device (Signa HDx; GE Medical Systems) with 8US TORSOPA coil. The following sequences were used: axial T1-weighted fast spoiled gradient-echo sequence (Repetition time [TR]/Echo time [TE], 230 ms/2.424 ms; matrix, 320×170; field of view [FOV], 38 cm; slice thickness, 6 mm; space, 2 mm); axial fat-suppressed respiratory-triggered fast spin-echo T2-weighted sequences [TR/TE, 6315.8 ms/85.2 ms; matrix, 320×224; FOV, 38 cm; number of excitation [NEX], 2; slice thickness, 6 mm; space, 2 mm); single-shot echo-planar imaging (SS-EPI) monoexponential DWI sequence (b value 0, 800 s/mm^2; TR/TE, 1825 ms/62.3 ms; matrix, 96×130; FOV, 38 cm; NEX, 5; slice thickness, 6 mm; space, 2 mm); SS-EPI multiple b values DWI sequence (b values 0, 20, 50, 100, 150, 250, 400, 600, 800, 1000 s/mm^2; TR/TE, 4000 ms/71.1 ms; matrix, 128×128; FOV, 38 cm; NEX 2; slice thickness, 6 mm; interscan space, 2 mm; acquisition time, 252 s). The image noise was reduced by array spatial sensitivity encoding technique in all patients before scan. A dynamic contrast-enhanced MRI (DCE-MRI) was applied at last with liver acceleration volume acquisition sequence (TR/TE, 2.964 ms/1.36 ms; matrix, 256×180; FOV, 42 cm; slice thickness, 2.5 mm; no interscan gap). The gadopentetate dimeglumine (Magnevist; Bayer Schering Pharma AG) was administered at a dose of 0.1 mL/kg body weight, and the flow velocity was 2 mL/s.

Image processing

All images were processed by two senior radiologists on an Advantage Windows workstation (ADW 4.3, GE Healthcare); the observers were unaware of the pathologic finding. The monoexponential and biexponential model parameters were all measured in multiple b values DWI sequence to make sure that the size and shape of the regions of interest (ROIs) were all the same. Color maps were generated automatically. The ROI was placed at a solid area of the tumor at the central level on multiple b values DWI sequence b=0 images. Then, ROIs were automatically placed in the same area on different b value images, on monoexponential and biexponential parameters maps. The ROIs were either circular or elliptical, 30–120 mm^2 in size. Since the DWI signal intensity acquired for ADCf and *f* values may occasionally exceed the range of the calculation, regions of remarkable overflow were avoided during ROI placement. On this basis, the size of ROI was kept as large as possible in the solid part. To avoid cysts and necrotic areas, we overlaid conventional MRI sequences (T2-weighted imaging and DCE-MRI) with diffusion-weighted images. The values of ROIs of all the parameters were measured three times, and the mean values were adopted. ROIs were also placed in normal cortical areas as control; the ROIs were either circular or elliptical to best fit the shape to the normal area of renal cortex, covering an area no less than 30 mm^2. All parameters were automatically calculated at the workstation.

The equation for the monoexponential model was as follows:

$S2/S1 = \exp(-bADC)$

Where b is the diffusion-weighting factor, S2 and S1 are the signal strengths of tissues at high b values and at b=0 s/mm^2, and ADC is the apparent diffusion coefficient.

Biexponential DWI parameters were calculated using the formula:

$S/S0 = f\exp(-bADCf) + (1 - f)\exp(-bADCs)$

Where S and S0 are the signal strengths at a particular b value and b=0 s/mm^2, *f* is the fraction of ADCf, ADCf (fast apparent diffusion coefficient) is the diffusion constant of pseudodiffusion component, and ADCs (slow apparent diffusion coefficient) is the diffusion constant of pure diffusion component (23).

Statistical analysis

STATA 10.0 software (Stata Corp. LP) was used to analyze all data. Statistics were presented as mean±standard deviation or median (min–max). Correlation between all parameters of both models and the Fuhrman nuclear grading was analyzed using Spearman's rank correlation. Patients were assigned into two groups according to their Fuhrman nuclear grading: low-grade (grades I and II) and high-grade (grades III and IV). Bartlett test was employed to analyze normal distribution and homogeneity of variance. Independent samples t-test was performed to compare parameters of the two groups. Receiver operating characteristic (ROC) curves of all parameters were created; area under the ROC curve (AUC) was used to determine the effectiveness of ADC and biexponential parameters for distinguishing the tissues of the two groups. Z test was used for pairwise comparisons between the AUCs of ADC and biexponential parameters. Maximum Youden index (J) was used to determine the optimal sensitivity and specificity, and the corresponding diagnostic cutoff point. $P < 0.05$ was considered significant.

Results

The median age of the enrolled 33 patients was 54 years (range, 30–75 years). The mean tumor diameter was 42.70±15.06 mm. A total of 21 patients had tumor in the right kidney, whereas 12 patients had tumor in the left kidney. Only one patient had a Fuhrman nuclear grade I tumor, 14 had grade II tumors, 16 had grade III tumors, and two had grade IV tumors. Due to the small number of patients with Fuhrman grade I and IV tumors, we classified grades I and II as low-grade, while grades III and IV as high-grade. Low- and high-grade groups had a median age of 52 years (range, 30–68 years) and 61.5 years (range, 38–75 years), respectively.

Table 2. Correlation of monoexponential and biexponential DWI parameters with the Fuhrman nuclear grading of tumors

	ADCf	ADCs	*f* value	$ADC_{0\text{-}800}$
r	0.779	-0.607	0.548	-0.553
P	<0.001	<0.001	0.001	0.001

ADCf, fast apparent diffusion coefficient; ADCs, slow apparent diffusion coefficient; f value, fraction of ADCf; $ADC_{0\text{-}800}$, apparent diffusion coefficients of b value (0, 800 s/mm^2); r, correlation coefficient.

Table 3. Monoexponential and biexponential DWI parameters of Fuhrman low- and high-grade tumors

	ADCf (×10^{-3} mm^2/s)	ADCs (×10^{-3} mm^2/s)	*f* value (%)	$ADC_{0\text{-}800}$ (×10^{-3} mm^2/s)
Fuhrman low-grade tumors	24.01±11.2	1.36±0.29	24.4±5.57	1.89±0.21
Fuhrman high-grade tumors	65.63±26.4	1.11±0.17	36.31±10.43	1.64±0.29
P	<0.001	0.005	<0.001	0.009

ADCf, fast apparent diffusion coefficients; ADCs, slow apparent diffusion coefficients; $ADC_{0\text{-}800}$, apparent diffusion coefficients of b value (0, 800 s/mm^2); *f* value, fraction of ADCf.

Table 4. AUC analysis of biexponential DWI parameters and corresponding sensitivity, specificity, and accuracy in prediction of Fuhrman low- and high-grade tumors

	ADCf	ADCs	*f* value	$ADC_{0\text{-}800}$
AUC	0.959	0.807	0.833	0.789
Maximum Youden index (J)	0.889	0.633	0.778	0.533
Best diagnostic cutoff (×10^{-3} mm^2/s)	39.5	1.25	33.2	1.74
Sensitivity (%)	88.9	83.3	77.8	86.7
Specificity (%)	100	80.0	100	66.7
Accuracy (%)	93.94	81.8	87.9	75.8

AUC, area under the ROC curve; DWI, diffusion-weighted imaging; ADCf, fast apparent diffusion coefficient; ADCs, slow apparent diffusion coefficient; *f* value, fraction of ADCf; $ADC_{0\text{-}800}$, apparent diffusion coefficient of b value (0, 800 s/mm^2).

Monoexponential ADC values had a negative correlation with the nuclear grade of tumors (correlation coefficient r, -0.553; $P = 0.001$). We found a stronger correlation between biexponential parameters and Fuhrman nuclear grading of tumors. The correlation coefficient of ADCf was 0.779 ($P < 0.001$), ADCs was -0.607 ($P < 0.001$), but *f* value was only 0.548 ($P = 0.001$). ADCf and *f* were positively correlated, while ADCs negatively correlated with the nuclear grade of tumors. Compared with other parameters obtained from both models, ADCf had the closest correlation with Fuhrman nuclear grading (Table 2).

High-grade ccRCC showed remarkably lower monoexponential ADC than low-grade ccRCC. The AUC for the differential diagnosis of low- and high-grade tumors was 0.789, the best cutoff point was 1.74×10^{-3} mm^2/s, and the sensitivity and specificity were 86.7% and 66.7%, respectively.

High-grade ccRCC showed markedly higher ADCf and *f* value but lower ADCs than low-grade ccRCC (Figs. 1 and 2), with significant differences ($P < 0.05$) (Table 3). The AUCs of ADCf, ADCs, and *f* curves were 0.959, 0.807, and 0.833, respectively. The ADCf showed a higher AUC than other parameters, with a relatively higher diagnostic sensitivity and specificity (Table 4), but the difference failed to reach a statistically significance ($P = 0.101$ for ADCf vs. *f* and $P = 0.089$ for ADCf vs. ADCs).

The AUC of ADCf was also superior to that of monoexponential ADC values, and the difference reached statistical significance, but the *P* value was just a little lower than 0.05 ($P = 0.046$). Thus, a larger group of samples is required to further verify its diagnostic efficiency. In addition, the AUC of ADCs and *f* showed no significant difference from ADC ($P = 0.850$ for ADCs vs. ADC and $P = 0.739$ for *f* vs. ADC).

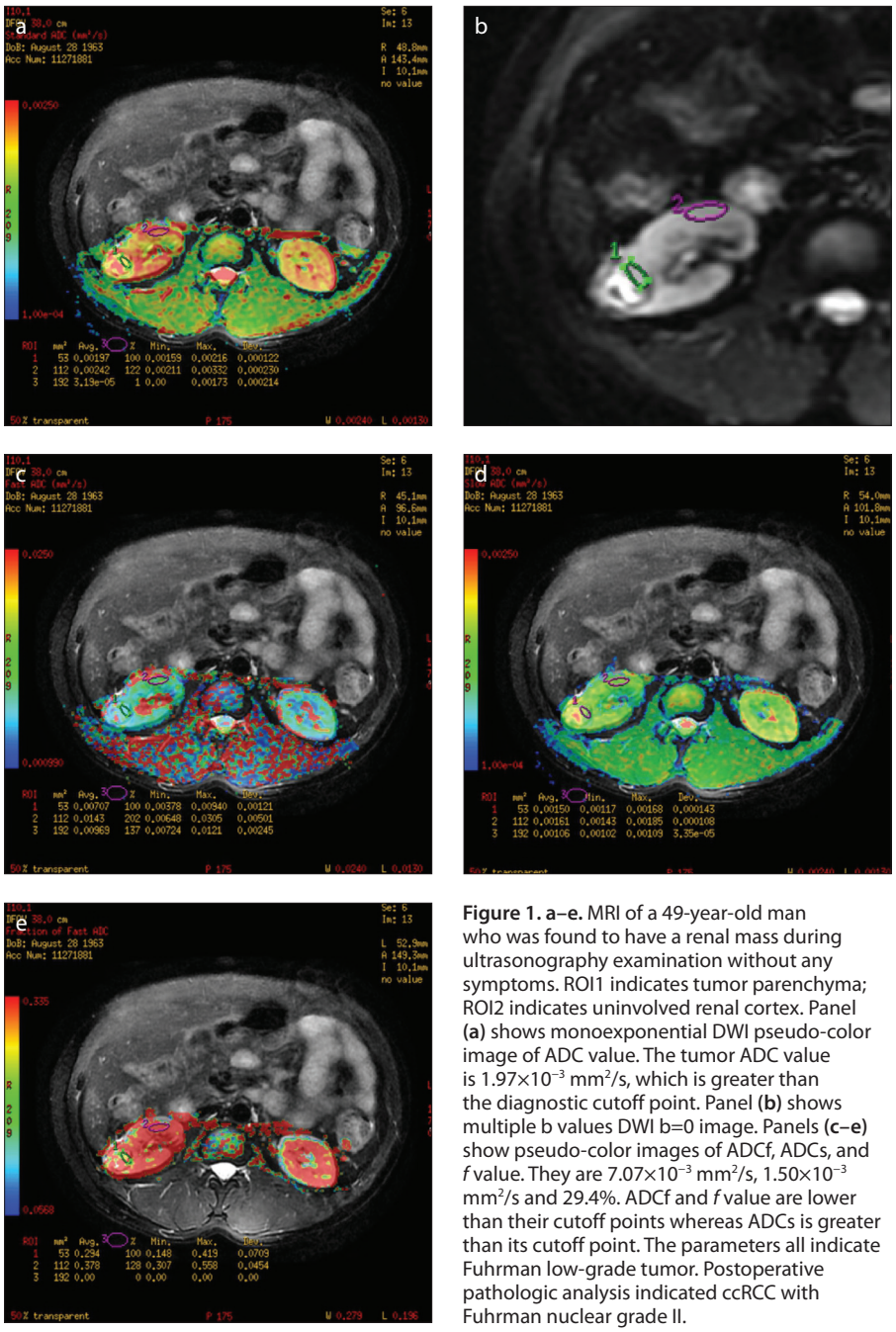

Figure 1. a–e. MRI of a 49-year-old man who was found to have a renal mass during ultrasonography examination without any symptoms. ROI1 indicates tumor parenchyma; ROI2 indicates uninvolved renal cortex. Panel **(a)** shows monoexponential DWI pseudo-color image of ADC value. The tumor ADC value is 1.97×10^{-3} mm^2/s, which is greater than the diagnostic cutoff point. Panel **(b)** shows multiple b values DWI b=0 image. Panels **(c–e)** show pseudo-color images of ADCf, ADCs, and *f* value. They are 7.07×10^{-3} mm^2/s, 1.50×10^{-3} mm^2/s and 29.4%. ADCf and *f* value are lower than their cutoff points whereas ADCs is greater than its cutoff point. The parameters all indicate Fuhrman low-grade tumor. Postoperative pathologic analysis indicated ccRCC with Fuhrman nuclear grade II.

Discussion

Our study demonstrates that discrimination of high or low Fuhrman grade of ccRCC is feasible by both monoexponential and biexponential DWI. All parameters of both models were significantly correlated with Fuhrman grade. The patients with high grade were determined with a dominant decrease in tumor diffusivity (reflected by lower ADC or ADCs). And high grade tumors had higher ADCf and f, which might indicate more heterogeneity and complexity of microvasculature in high grade tumors. Moreover, the ADCf revealed a higher AUC than ADC value. Our results indicate that biexponential DWI may contribute to the characterization of Fuhrman grade of ccRCC.

The ccRCC is a highly malignant subtype of renal cancer with a poor prognosis (24). Fuhrman grading system classifies tumors into four grades according to nuclear size, nuclear shape, and nucleolar prominence (3). A study involving 634 patients with RCC by Tsui et al. (25) showed that the five-year survival rates were 89% for grade I tumors, 65% for grade II tumors, but only 46% for grade III and IV tumors. It is clear that the Fuhrman grading system is important to predict the aggressiveness and prognosis of ccRCC. Previously, preoperative diagnosis of Fuhrman grade was achieved via biopsy. However, Campbell et al. (4) suggested that percutaneous core biopsies were invasive and could be nondiagnostic in 2.5% to 22% of cases due to sampling failure. Recently, functional MRI has began to be used for RCC because it is noninvasive and reproducible. Gurel et al. (7) showed that histopathologic characterization of renal masses with MRI was superior to percutaneous biopsy, and suggested that conventional MRI in addition with ADC values might improve tissue characterization.

The monoexponential DWI is commonly used in clinical practices and researches. Sandrasegaran et al. (8) reported that high-grade tumors had lower ADC than low-grade ones, but there was no statistically significant difference between them. However, Goyal et al. (9) found a significant difference, and Yu et al. (10) demonstrated that the ADC values of different grades of ccRCC were significantly different except grade I vs. II and grade III vs. IV. We also found statistically significant difference between the ADC values of high- and low-grade tumors. Variation in the results of these studies might be related to different scanners, scanning parameters, and different sample sizes.

There have been some studies attempting to apply biexponential model in clinical practice (15–22). Biexponential model not only enables the quantitative measurement of tissue diffusivity, but also distinctly isolates microcirculatory perfusion effects from tissue diffusivity, which is unavailable from the monoexponential model. It has been demonstrated to be better for the characterization of water diffusion decay in the nervous system and prostate than the monoexponential model (19–22). In the kidney, Chandarana et al. (17) showed that it could discriminate enhancing renal lesions from nonenhancing ones in the absence of contrast agents. Moreover, Chandarana et al. (15) differentiated between subtypes of renal neoplasms using biexponential fitting of DWI, and found that the combination of the *f* value and ADCs had an accuracy of 86.5% in discriminating ccRCC and chromophobe RCC. In addition, their study confirmed significantly strong correlation between the *f* value and the cumulative initial area under the curve of gadolinium concentration at 60 seconds (CIAUC60) which reflects tumor perfusion.

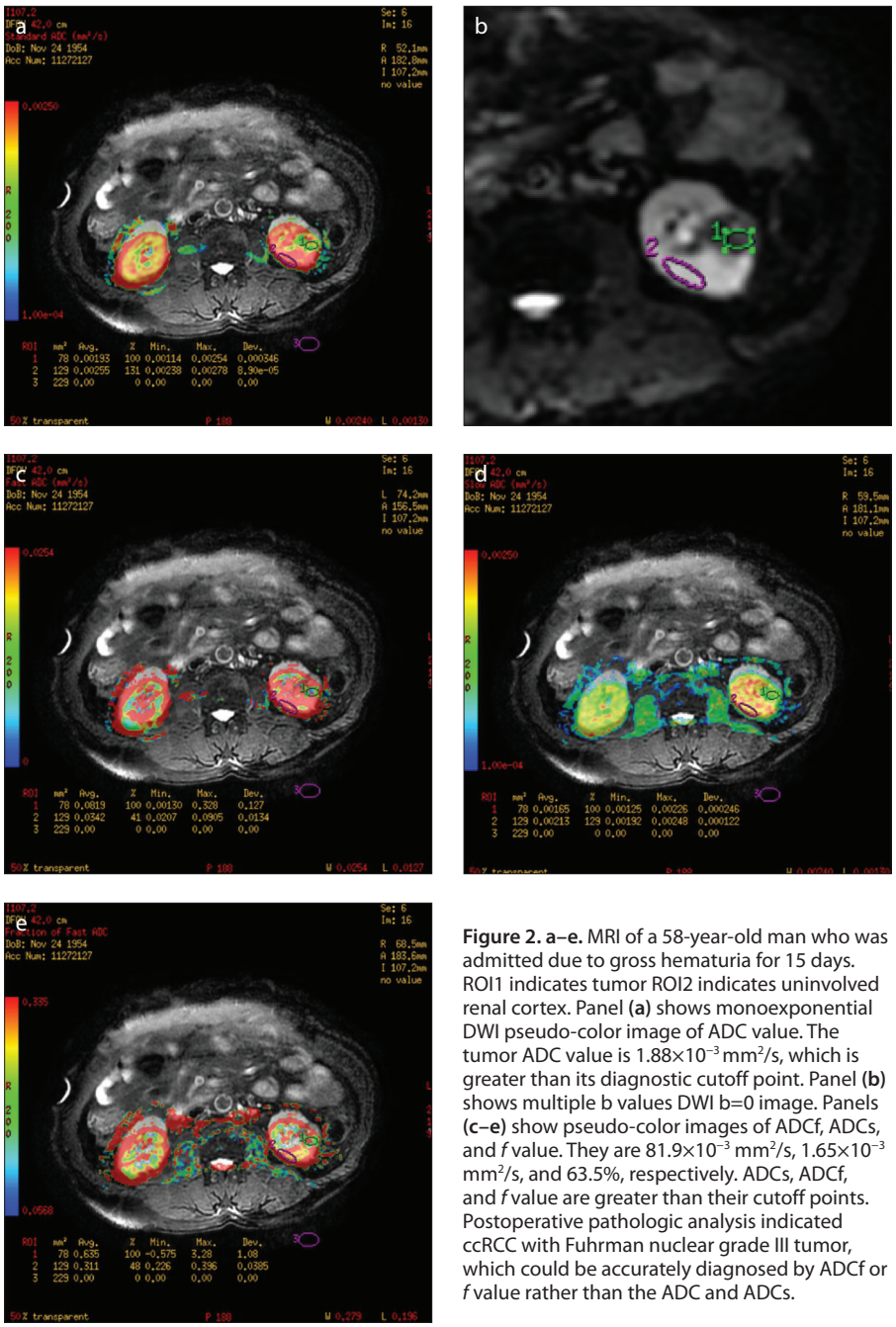

Figure 2. a–e. MRI of a 58-year-old man who was admitted due to gross hematuria for 15 days. ROI1 indicates tumor ROI2 indicates uninvolved renal cortex. Panel **(a)** shows monoexponential DWI pseudo-color image of ADC value. The tumor ADC value is 1.88×10^{-3} mm^2/s, which is greater than its diagnostic cutoff point. Panel **(b)** shows multiple b values DWI b=0 image. Panels **(c–e)** show pseudo-color images of ADCf, ADCs, and *f* value. They are 81.9×10^{-3} mm^2/s, 1.65×10^{-3} mm^2/s, and 63.5%, respectively. ADCs, ADCf, and *f* value are greater than their cutoff points. Postoperative pathologic analysis indicated ccRCC with Fuhrman nuclear grade III tumor, which could be accurately diagnosed by ADCf or *f* value rather than the ADC and ADCs.

Thus far, biexponential DWI had limited clinical applications in determination of Fuhrman nuclear grade of renal tumors. Only Rheinheimer et al. (18), in their study involving 20 patients with ccRCC, reported a weak but significant correlation between the Fuhrman nuclear grade and the *f* value (r=0.54) and ADCs (r=0.51). High-grade ccRCC had higher *f* value and lower ADCs compared with low-grade, consistent with our results. But no statistically significant correlation was found in their study for ADCf. This finding was inconsistent with our results, which showed higher positive correlation coefficients between the ADCf and the Fuhrman nuclear grade. Michaely et al. (26) indicated that tumor growth increased with higher tumor grade. As tumor grows, original capillaries cannot satisfy the growth requirements, more blood vessels are generated in the tumor tissue, leading to increased microcapillary density, tumor blood flow, and relative blood volume of the tumor. This may result in remarkable differences in the tumor tissue perfusion components between low- and high-grade tumors, and it might explain the increase in ADCf and *f* value, along with increasing Fuhrman nuclear grade. Since ADCf is closely related with tissue perfusion, *f* value, which represents the fraction of ADCf, is also related with tissue perfusion. Many studies have already confirmed the correlation between *f* value and the degree of tumor enhancement or perfusion components (15, 17).

There was no significant difference between the parameters of the low- and high-grade tumor groups in Rheinheimer et al. (18). This was inconsistent with our results. The possible reasons could be variations in the sample size, equipment, and b values between the studies. In their study, MRI examinations were performed on 20 patients using a 1.5 Tesla MRI. They used less number of b values (0, 50, 100, 150, 200, 300, 400, 600, 800 s/mm^2) and a relatively lower maximal b value compared with ours and the sample sizes of both studies were small, which may have contributed to the different results in the two studies.

This study had some limitations. First, our sample size was small. Larger studies are needed for further investigation. Second, due to longer DWI time biexponential fitting was more susceptible to motion artifacts, particularly for tumors located at the lower pole. Third, the ROIs were mostly placed within the tumor parenchyma, but some tumors contained unevenly distributed cysts; thus some small cystic components could not be avoided within the ROI. Lastly, the size of ROIs in our study ranged widely due to tumor size variations. Thus, the heterogeneity of a larger tumor may have been greater than a smaller tumor (e.g., some minimal necrosis could have been included), leading to some bias in measurements.

In conclusion, biexponential DWI has a slight advantage over monoexponential DWI in differentiating between Fuhrman high- and low-grade RCCs. Biexponential DWI provides more parameters and the ADCf performs a little better than ADC. We suggest that this may be a potential diagnostic technique in future studies.

Acknowledgements

The authors would like to thank Jian Mao and Lei Yue in the Department of Radiology of Shanghai Cancer Center for the MRI scanning. The authors thank He Wang in the Global Applied Science Laboratory of GE Healthcare for his help in image processing.

Conflict of interest disclosure

The authors declared no conflicts of interest.

References

1. Gupta K, Miller JD, Li JZ, et al. Epidemiologic and socioeconomic burden of metastatic renal cell carcinoma (mRCC): a literature review. Cancer Treat Rev 2008; 34:193–205. [CrossRef]

2. Jemal A, Siegel R, Ward E, et al. Cancer statistics 2009. CA Cancer J Clin 2009; 59:225–249. [CrossRef]
3. Minardi D, Lucarini G, Mazzucchelli R, et al. Prognostic role of Fuhrman grade and vascular endothelial growth factor in pT1a clear cell carcinoma in partial nephrectomy specimens. J Urol 2005; 174:1208–1212. [CrossRef]
4. Campbell N, Rosenkrantz AB, Pedrosa I. MRI phenotype in renal cancer: is it clinically relevant. Top Magn Reson Imaging 2014; 23: 95–115. [CrossRef]
5. Türkvatan A, Akdur PO, Altinel M, et al. Preoperative staging of renal cell carcinoma with multidetector CT. Diagn Interv Radiol 2009; 15: 22–30.
6. Bata P, Gyebnar J, Tarnoki DL, et al. Clear cell renal cell carcinoma and papillary renal cell carcinoma: differentiation of distinct histological types with multiphase CT. Diagn Interv Radiol 2013; 19: 387–392. [CrossRef]
7. Gurel S, Narra V, Elsayes KM, et al. Subtypes of renal cell carcinoma: MRI and pathological features. Diagn Interv Radiol 2013; 19: 304–311. [CrossRef]
8. Sandrasegaran K, Sundaram CP, Ramaswamy R, et al. Usefulness of diffusion-weighted imaging in the evaluation of renal masses. AJR Am J Roentgenol 2010; 194: 438–445. [CrossRef]
9. Goyal A, Sharma R, Bhalla AS, et al. Diffusion-weighted MRI in renal cell carcinoma: a surrogate marker for predicting nuclear grade and histological subtype. Acta Radiologica 2012; 53:349–358. [CrossRef]
10. Yu X, Lin M, Ouyang H, et al. Application of ADC measurement in characterization of renal cell carcinomas with different pathological types and grades by 3.0T diffusion-weighted MRI. Eur J Radiol 2012; 81: 3061–3066. [CrossRef]
11. Zhang J, Tehrani YM, Wang L, et al. Renal masses: characterization with diffusion-weighted MR imaging--a preliminary experience. Radiology 2008; 247:458–464. [CrossRef]
12. Wang H, Cheng L, Zhang X, et al. Renal cell carcinoma: diffusion-weighted MR imaging for subtype differentiation at 3.0 T. Radiology 2010; 257: 135–143. [CrossRef]
13. Taouli B, Thakur RK, Mannelli L, et al. Renal lesions: characterization with diffusion-weighted imaging versus contrast-enhanced MR imaging. Radiology 2009; 251:398–407. [CrossRef]
14. Squillaci E, Manenti G, Di SF, et al. Diffusion-weighted MR imaging in the evaluation of renal tumours. J Exp Clin Cancer Res 2004; 23:39–45.
15. Chandarana H, Kang SK, Wong S, et al. Diffusion-weighted intravoxel incoherent motion imaging of renal tumors with histopathologic correlation. Invest Radiol 2012; 47:688–696. [CrossRef]
16. Heusch P, Wittsack HJ, Pentang G, et al. Biexponential analysis of diffusion-weighted imaging: comparison of three different calculation methods in transplanted kidneys. Acta Radiol 2013; 54:1210–1217. [CrossRef]
17. Chandarana H, Lee VS, Hecht E, et al. Comparison of biexponential and monoexponential model of diffusion weighted imaging in evaluation of renal lesions: preliminary experience. Invest Radiol 2011; 46:285–291.
18. Rheinheimer S, Stieltjes B, Schneider F, et al. Investigation of renal lesions by diffusion-weighted magnetic resonance imaging applying intravoxel incoherent motion-derived parameters-initial experience. Eur J Radiol 2012; 81:e310–316. [CrossRef]
19. Liu X, Peng W, Zhou L, et al. Biexponential apparent diffusion coefficients values in the prostate: comparison among normal tissue, prostate cancer, benign prostatic hyperplasia and prostatitis. Korean J Radiol 2013; 14:222–232. [CrossRef]
20. Brugieres P, Thomas P, Maraval A, et al. Water diffusion compartmentation at high b values in ischemic human brain. AJNR Am J Neuroradiol 2004; 25:692–698.
21. Shinmoto H, Oshio K, Tanimoto A, et al. Biexponential apparent diffusion coefficients in prostate cancer. Magn Reson Imaging 2009; 27:355–359. [CrossRef]
22. Zhang Y, Wang Q, Wu C, et al. The histogram analysis of diffusion-weighted intravoxel incoherent motion (IVIM) imaging for differentiating the gleason grade of prostate cancer [J]. Eur Radiol 2015; 25:994–1004. [CrossRef]
23. Le BD, Breton E, Lallemand D, et al. Separation of diffusion and perfusion in intravoxel incoherent motion MR imaging. Radiology 1988; 168:497–505. [CrossRef]
24. Escudier B, Eisen T, Stadler WM, et al. Sorafenib in advanced clear-cell renal-cell carcinoma. N Engl J Med Overseas Ed 2007; 356:125–134. [CrossRef]
25. Tsui KH, Shvarts O, Smith RB, et al. Prognostic indicators for renal cell carcinoma: a multivariate analysis of 643 patients using the revised 1997 TNM staging criteria. J Urol 2000; 163:1090–1095. [CrossRef]
26. Michaely HJ, Kramer H, Oesingmann N, et al. Intraindividual comparison of MR-renal perfusion imaging at 1.5 T and 3.0 T. Invest Radiol 2007; 42:406–411. [CrossRef]